Theory of carbon nanotube growth

A. Maiti, C. J. Brabec, C. Roland, and J. Bernholc
Department of Physics, North Carolina State University, Raleigh, North Carolina 27695
(Received 5 July 1995)

The kinetics of carbon nanotube growth under arc discharge conditions were investigated over different length and time scales using complementary numerical techniques. Relaxation by *ab initio* molecular dynamics (Car-Parrinello method) shows that large electric fields present at the tube tips are not the critical factor responsible for the open-ended growth observed experimentally. Classical molecular-dynamics simulations using realistic many-body carbon-carbon potentials show that wide tubes that are initially open can continue to grow straight and maintain an all-hexagonal structure. However, tubes narrower than a critical diameter, estimated to be about ~3 nm, readily nucleate curved, pentagonal structures that lead to tube closure with further addition of atoms. Very narrow tubes can be grown, however, if a small metal particle prevents tube closure. This effect was simulated explicitly by kinetic Monte Carlo methods. Monte Carlo simulations were also used to study nanotube growth over longer time scales. The resulting structures are in agreement with the above growth scenario, and provide an estimate for the lowest tube tip temperature necessary for the growth of nanotubes.

I. INTRODUCTION

Carbon is a rare element that possesses the ability to form a wide variety of networklike sp^2-bonded structures, generically termed fullerenes. These structures can be looked upon as graphitic sheets that have been curved in order to eliminate the dangling bonds. After the initial discovery of C_{60},[1] and particularly following the synthesis of C_{60} in macroscopic quantities in an arc discharge,[2] fullerene research has gained considerable momentum. A large number of different networklike structures have since been discovered. These include single carbon cages other than C_{60},[3–5] multishell fullerenes,[6,7] and carbon nanotubes.[8–10] Recently, the field of nanotubes has been the subject of intense research, in anticipation of novel technological applications. The high length-to-diameter ratio over which the nanotubes maintain a perfect hexagonal atomic arrangement makes them ideal candidates as superstrong fibers. The tubes also display unusual structural and electronic properties as a function of diameter and helicity, showing substantial promise as composites, catalysts, molecular wires, and molecular switches.[11–14]

Carbon nanotubes consist of concentric cylinders of a hexagonal (graphitic) network arranged around each other with a helical twist. In a carbon arc discharge apparatus, bundles of coaxial nanotubes of diameters ranging between 2 and 20 nm form at the negative electrode.[8,9] Single-shell nanotubes of diameters between 1 and 3 nm have also been synthesized by using metal catalysts[15] and through the plasma decomposition of benzene.[16]

If carbon nanotubes are ever to fulfill their technological promise, one must be able to fabricate them in bulk quantities. An understanding of their growth kinetics is therefore crucial. This is a problem of considerable complexity, since nanotubes form under highly nonequilibrium conditions. While it was initially believed that nanotube growth takes place through the addition of adatoms to the tips of closed tubes,[17] experiments show that the tube remains open during growth.[10] This is surprising, because the large number of dangling bonds definitely favors energetically a saturated, and therefore closed, sp^2 geometry. Moreover, the closed growth model cannot explain the growth of the inner shells of a multishell tube, because the supply of atomic deposits to the inner shells should be cut off by the closed cap of the outer shell. Thus the key question is, what keeps the carbon nanotube open during growth?

A number of possibilities have been conjectured to explain open-ended nanotube growth. Temporary saturation of dangling bonds by hydrogen is a possibility. However, hydrogen is almost completely excluded in the arc discharge experiments producing the nanotubes.[9] A large thermal gradient at the tube tip might also give rise to nonequilibrium forces that could favor the open geometry. However, as argued by Smalley,[18] at 500 Torr of He pressure[9] and a high temperature of 4000–5000 K at the center of the arc, collisions will quickly establish equilibrium between the electrons, the positive and neutral carbon atoms, and the clusters. This precludes the possibility of a temperature gradient large enough to affect the strong carbon bonds at the tube tip. However, as discussed in the next section, nanotubes in an arc discharge form in a region with large electric fields. Because of the large aspect ratio, metallic nanotubes effectively behave as sharp antennas, and can further intensify the field at their tips. It has therefore been postulated that large electric fields at the tips of growing nanotubes (of the order of 1 V/Å) are responsible for keeping them open.[18]

In this paper, we present the results of an extensive theoretical study of the growth of carbon nanotubes in an

arc discharge, using a variety of complementary numerical methods. Our *ab initio* molecular-dynamics (MD) calculations show that, surprisingly, the electric field alone cannot stabilize an open-ended structure, even for very narrow tubes. This naturally leads to a study of the kinetics of nanotube growth, which we have investigated with classical MD simulations. Because of the inherent mismatch between accessible simulation times for classical MD simulations (nanoseconds) and the long experimental growth times (milliseconds), it is not possible at present to simulate the large-scale growth of carbon nanotubes directly, at least not without assuming unrealistically large deposition rates. Generally, such large deposition rates lead to the formation of structural defects that do not anneal out over the time scales of a MD simulation, and therefore only yield a disordered tube structure. Our approach has therefore been to use MD simulations to study the microscopic aspects of tube growth, i.e., MD simulations were used to identify and classify all possible adatom structures, their annealing times, and subsequent dynamics. The relevant growth structures and their kinetics were then incorporated into a kinetic Monte Carlo code, which was used to simulate the growth of carbon nanotubes at rates approaching the experimental time scales.

The organization of this paper is as follows. In Sec. II we calculate and discuss the role of electric field in keeping the nanotubes open during growth. In Sec. III we describe classical MD simulations of nanotube growth and identify the key bond-switching and ring migration processes. In Sec. IV we discuss the implementation of the kinetic Monte Carlo formalism, the results of these simulations, and give an estimate of the minimum temperature necessary for nanotube growth. We also simulate the effect of small metal particles in facilitating the growth of narrow tubes. We conclude with a summary in the final Sec. V.

II. ROLE OF ELECTRIC FIELD

To assess the role of the electric field **E**, we first solve for the field present at the tips of open and closed nanotubes in an arc discharge. The effect of such a field on the energies of both open and closed tubes is then studied with *ab initio* MD simulations. Surprisingly, an unrealistically long tube length is required before the electric field alone can stabilize the growth of an open tube.

To solve for the appropriate electric field, it is first necessary to analyze the experimental setup in which the nanotubes are formed. The arc discharge apparatus consists of a carbon arc with a potential drop of 20–30 V across a 1-mm gap between two rod-shaped graphite electrodes, each with a diameter of several millimeters. The reaction vessel confining the arc is filled with an inert gas, usually He, at a pressure of 100–500 Torr. A plasma sheath, primarily consisting of carbon ions, forms adjacent to the graphite cathode, on which the nanotubes grow.[19] The thickness of the sheath is about 100 nm, and the potential drop across it is equal to the ionization potential of carbon, roughly 10 V. The growing nanotubes are thus immersed in a uniform field of ~ 0.01 V/Å, leading to a geometry depicted in Fig. 1.

In order to calculate the electric field at and around the tube tip, we integrated Laplace's equation for the arc discharge geometry described above (see also Fig. 1), with the tubes modeled as continuous metallic rods. The closed tube of length L and radius R consists of a cylinder of length $(L-R)$ capped by a hemisphere of radius R. The open tube is represented by two cylinders of radii $(R-\delta)$ and $(R+\delta)$ and a common length $(L-\delta)$, with their rims joined by a half torus of radius δ [Fig. 1(b)]. The thickness 2δ of an open tube is taken to be 1 Å, independent of the tube length and radius. The boundary conditions consist of $V=0$ at all points of the cathode and on the nanotube, $V=10$ V at all points on the effective "anode" (corresponding to the top layer of the plasma adjoining the cathode), and the horizontal component of the electric field being zero at every point of the axis of the nanotube. A variable-sized triangular mesh was used for all calculations in order to ensure a high numerical accuracy, particularly close to the tip. For the above geometry, Laplace's equation was solved numerically in two-dimensional cylindrical coordinates (because of the azimuthal symmetry around the tube

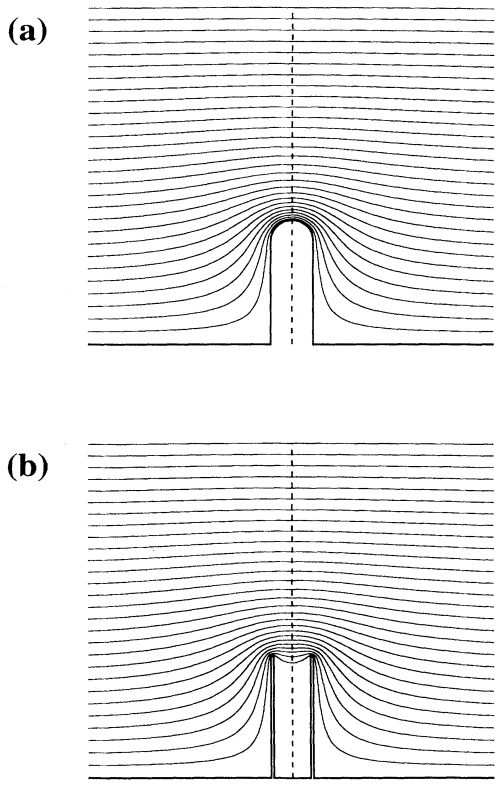

FIG. 1. Cylindrical cross section of geometries used for the calculation of the electric field distribution for (a) a closed tube and (b) an open tube. The actual three-dimensional (3D) geometry is obtained by rotating the figures about the tube axis. The equipotential lines are indicated by solid lines.

axis), using the finite difference program POISSON from Los Alamos.[20] As shown by the equipotential lines in Figs. 1(a) and 1(b), there is a considerable enhancement of electric field at the tips of both the open and the closed tubes, but more so for the open tubes. However, the electrostatic potential distribution for the open and the closed tubes of the same L and R differ only in the vicinity of their tips and are practically identical a few radii away from the tips. This is more apparent if one compares the surface charge densities of an open and a closed tube as a function of the vertical distance from the tube tip (Fig. 2). Our calculated values for the electric fields at the tips of *closed* and *open* tubes of various lengths and diameters are well fitted by the formulas

$$E_{\text{tip,closed}} = E_0 \left[0.87 \frac{L}{R} + 4.5 \right]$$

and

$$E_{\text{tip,open}} = E_0 \left[2.35 R^{0.65} \frac{L}{R} + 4.55 \right],$$

where L and R are in nanometers. The above fits are valid within the ranges of $0.2 < R < 10$ nm, $20 < L < 60$ nm, and a ratio $L/R > 5$. For a closed tube, L and R are the only length scales of the problem, and thus $E_{\text{tip,closed}}$ depends only on the ratio L/R. For an open tube, however, the tube width 2δ (taken to be 1 Å) provides an additional length scale and this results in an explicit dependence of $E_{\text{tip,open}}$ on L and R. One should note that for both open and closed tubes of fixed length the electric field at the tip *decreases* as the tube diameter increases, and for a fixed diameter the electric field *increases* linearly with the length of the tube. However, even for the narrowest tube, with diameter 0.7 nm, the tube must grow to a length of $L_{\text{critical}} \sim 30$ nm before E_{tip} becomes ~ 1 V/Å, the estimated field strength required to influence a strong chemical bond.

To obtain a more accurate estimate of L_{critical}, the effects of the electric field on the tips of the nanotubes were investigated by the *ab initio* molecular-dynamics method of Car and Parrinello[21] with the ions being represented by a soft-core pseudopotential due to Li and Rabii.[22] The effect of the electric field was incorporated through the addition of an electrostatic energy term in both the electronic and ionic contributions to the total energy expression in the local density formulation. An energy cutoff of 26 Ry was used, corresponding to a basis set of 36 000 plane waves. The exchange-correlation functional was taken to be of the form given by Perdew and Zunger.[23] Tips of both open and closed tubes with a diameter of 0.7 nm were constructed. This small diameter was deliberately chosen so as to maximize the effects of the electric field and minimize the computational effort. As mentioned before, the electrostatic potentials for the open and the closed tubes differ only within a few radii from the tube tip. Therefore only a few atomic layers containing the tip are sufficient for comparing the energetic stability of the two tubes. In view of large memory requirements of the Car-Parrinello code, the above result is important, as it allows the comparison to be made with supercells of reasonable size. The open tube tip was constructed from six atomic layers of an armchair tube, known to be metallic,[14,24] while the closed tube was constructed by replacing the top three layers of the open tip by a hemispherical C_{60} cap. The supercell with the tips included a vacuum region 0.7 nm wide in all directions, so as to effectively isolate the tube tips from its periodic images. The electric field potential was convoluted by a smooth switching function across the vacuum region in order to preserve continuity with the periodic boundary conditions used in the Car-Parrinello code.

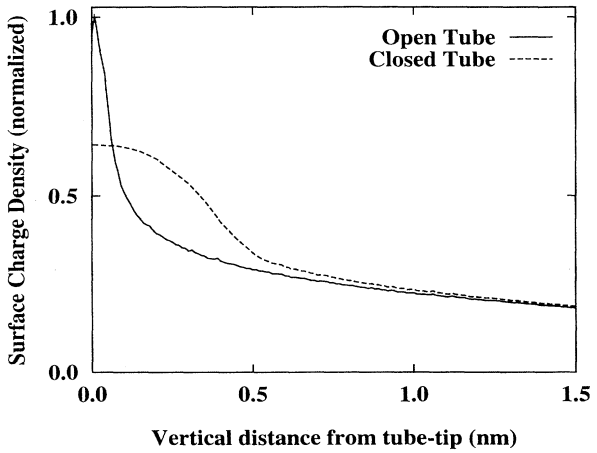

FIG. 2. Comparison of the surface charge densities at the tips of open and closed 0.7-nm-diam tubes.

Both tube tips were relaxed in the absence of any electric field. It was found that the presence of the dangling bonds at the open tube tip favors the closed tube geometry by 1.6 eV per dangling bond. As the electric field is turned on, the energies of both the open and the closed tubes decrease. In order to present the best possible case for the role of the electric field in enhancing open-ended growth, we neglected the electrostatic energy gain for the closed tube. We compared the energy of the open tube, which was electronically and structurally relaxed in electric fields calculated for several different lengths of the tube, with that of the closed tube at zero field. The total energy of the open tube tip was found to decrease linearly with a small quadratic component as a function of the tube length L. The crossover in stability from a closed to an open tube occurs at $L_{\text{critical}} \sim 49$ nm (Fig. 3), which corresponds to a field of ~ 1.7 V/Å at the tube tip. Since E_{tip} for a given L decreases with increasing tube diameter, one can expect that wider nanotubes will have an even larger L_{critical}. A nanotube of any reasonable diameter thus has to grow to an appreciable length before the electric field starts playing any significant role in keeping it open. Note that even if the nanotube attains the critical length by some growth mechanism, the electric field is still not likely to play a major role because of thermionic and field emission, which is expected to occur at field strengths smaller than ~ 1 V/Å.[19] The crossover field of 1.7 V/Å may therefore

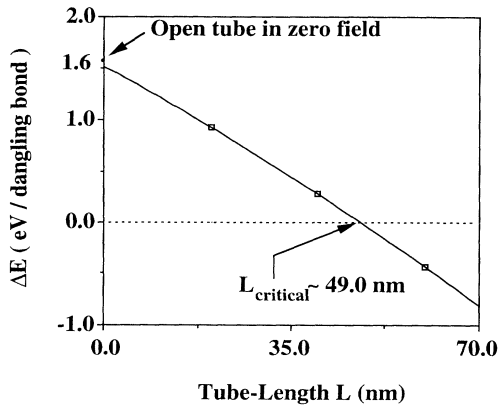

FIG. 3. The total energy of an open metallic tip of diameter 0.7 nm in the presence of an electric field as a function of tube length. The energy is normalized per dangling bond and measured relative to a closed tube of the same length and diameter in zero field. There is a stability crossover at a length ~49 nm.

not be attainable in practice.[25] We can therefore conclude that the electric field cannot be the critical factor responsible for keeping the tubes open during growth.

III. MOLECULAR-DYNAMICS SIMULATIONS OF NANOTUBE GROWTH

From the previous two sections it is clear that arguments based on temporary hydrogenation of dangling bonds, or the presence of thermal or electric potential gradients strong enough to favor an open tube geometry, can be ruled out under typical experimental conditions. Therefore it is natural to search for models based on the stability of local structures formed during growth. We have investigated the total energy of structures that form during deposition, and their subsequent dynamics, by means of classical MD simulations.

The carbon atoms in our MD simulations were modeled by the many-body Tersoff-Brenner potential,[26,27] which accurately reproduces the binding energies and elastic properties of a wide range of hydrocarbons and the bulk phases of carbon, i.e., diamond and graphite. For our growth simulations, a number of open tubes with varying diameters and helicities (n_1,n_2) were constructed (Fig. 4). A basic time step of 0.5 fs was used in a fifth-order Beeman-Verlet scheme to integrate the equations of motion. A nanotube length of about 12 Å was used in all the simulations. The tube tip was kept at the relatively high temperature of 3000 K, just below the melting point of graphite, in order to facilitate the annealing process. A linear temperature gradient was maintained along the length of the tube, with the bottom two layers being kept static. The temperature profile, defined as the average kinetic energy in a given layer, was maintained by a periodic renormalization of the atomic velocities every 2500 time steps. The electric field at the tube tip was assumed to focus the incoming carbon ions

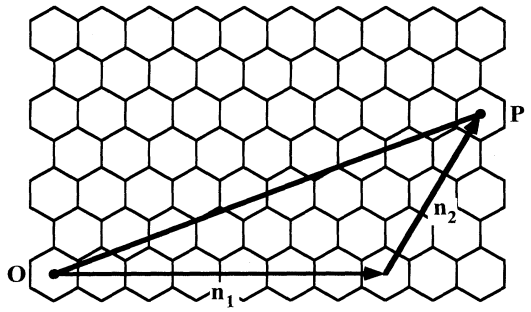

FIG. 4. Schematic illustration of the helicity notation used in this paper. A tube with helicity (n_1,n_2) is generated by wrapping a graphene sheet in such a fashion that the point $P(n_1,n_2)$ coincides with the origin. The resulting tube axis is normal to the line OP on the graphene sheet.

towards the tip of the growing nanotube. The energy of these incident ions depends not only on the electric field in the plasma but also on their state of ionization (i.e., singly or doubly charged) and the collisional patterns along their trajectories through the plasma. This uncertainty in the incident energy was modeled by aiming carbon atoms, dimers, and trimers randomly at different parts of the open tube edge with initial kinetic energies also varying randomly between 1 and 8 eV. As noted in our earlier work,[28,29] nanotube growth occurs by a net addition of dimers at the regions where a row of hexagons terminates at the tube tip, which we term the "step edge," as illustrated in Fig. 5.

Regardless of their initial energy, carbon atoms were always found to insert into the nearest ring, or form a pentagon at a step edge, for tubes wider than a critical diameter (to be discussed below). Dimers and trimers showed no unique pattern of deposition and their behavior included the insertion of all atoms into the same ring, the insertion of atoms into different rings, and starting a new layer by creating a newly exposed step edge. However, irrespective of the initially formed structures, the microscopic "annealing" processes involved bond switching and ring migration mechanisms that were the same in all cases. Therefore an analysis of the basic microscopic processes occurring at the nanotube tip based

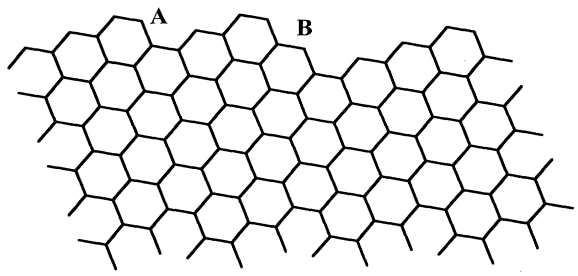

FIG. 5. A schematic of step edges at the tip of a helical nanotube. The points A and B denote single and double steps, respectively.

on simulations involving only the deposition of carbon atoms yields a comprehensive understanding of the nanotube growth kinetics.

Analysis of growth simulations on many different tubes leads to different scenarios of adatom addition for tube diameters larger and smaller than a critical value of ~3 nm. For the wider tubes, the incident atom always inserts into the nearest ring to form a larger ring or places itself at the step edge to form a new pentagonal ring. This insertion occurs within a few picoseconds at most, irrespective of the initial energy of the adatom. If the atom initially inserts into a hexagon (heptagon) away from a step edge, it forms a heptagon (octagon). Octagons are always energetically unstable and break up into smaller rings (two heptagons, or a heptagon and a hexagon if the octagon has a pentagon neighbor) by means of a single bond switch. Pentagons and heptagons formed at the tube tip migrate along a step by means of a series of single bond switches,[29] a prototypical example of which is shown in Fig. 6. They can also move to the adjoining step through single bond switches at the step edge. All single bond switches described above occur only at the tube tip and take place in a 10–100-ps time scale at 3000 K. From our detailed simulations it is clear that the initially formed heptagons and pentagons migrate and anneal into an essentially all-hexagonal structure, with the possible exception of a few isolated pentagons that get converted to hexagons by subsequent deposits. In reviewing our simulations we were able to categorize the various ways in which such annealing takes place in a wide tube, thereby allowing for open-ended growth: (a) a heptagon migrates to a step edge and breaks up into a pentagon and a hexagon [Fig. 7(a)]; (b) a heptagon "annihilates" with a pentagon to form a hexagon pair [Fig. 7(b)]; (c) a pentagon converts to a hexagon by the direct insertion of a deposited atom [Fig. 7(c)]; and (d) a pentagon pair at a step edge "fuses" together into a hexagon [Fig. 7(d)]. Note that processes (a) and (d) can occur only at a step edge, while processes (b) and (c) do not need the presence of a step edge.

For tubes narrower than the critical diameter the situation is very different. Total energy calculations of possible adatom structures, which included atomic relaxation, show that in these narrow tubes the hexagons at the step edges are not as stable energetically as adjacent pentagonal rings (see Ref. 28 and Table I below). Furthermore, pentagons separated by one or more hexagons are energetically more stable than a pair of adjacent pentagons (cf. the 565 or the 5665 configurations with the 55 configuration in Table I). Thus, once a hexagon at a step edge is converted to a pentagon pair (the configuration 55), the pentagons move away from each other and spread out over the tube edge. A large number of well-distributed pentagons at the tube tip gives rise to a curved geometry in which any additional deposited atom leads to the formation of a new ring, rather than inserting into an existing ring. These rings result in the formation of a cap that leads to tube closure with additional deposits. We tested the idea that a closed tube might grow by the addition of atoms and smaller clusters to the closed cap[17] by direct simulation. This only led to the formation of a disordered cap structure at the end of the tube, full of heptagonal and pentagonal defects. These defects do not anneal out within our simulation time.[29] We therefore conclude that nanotube growth can only occur for open-ended tubes wider than a critical diameter, estimated to be ~3 nm. This result is in agreement with the experimental observations of Iijima, Ajayan, and Ichihashi[10] and it also explains the conspicuous absence of tubes narrower than 2.2 nm in arc discharge experiments.[8]

So far, we have presented a consistent model for the growth and closure of a *single-walled* nanotube, while in general *multiwalled* tubes are formed in an arc discharge. However, once a single nanotube is formed, the next shell can readily grow using the surface as a template. If the

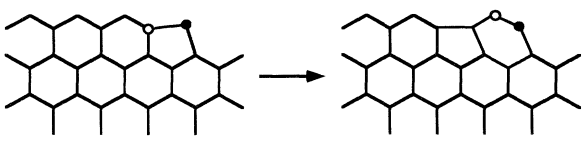

FIG. 6. A typical ring migration mechanism observed in MD simulations, illustrated here by the migration of a pentagon by a single bond switch at the tube tip.

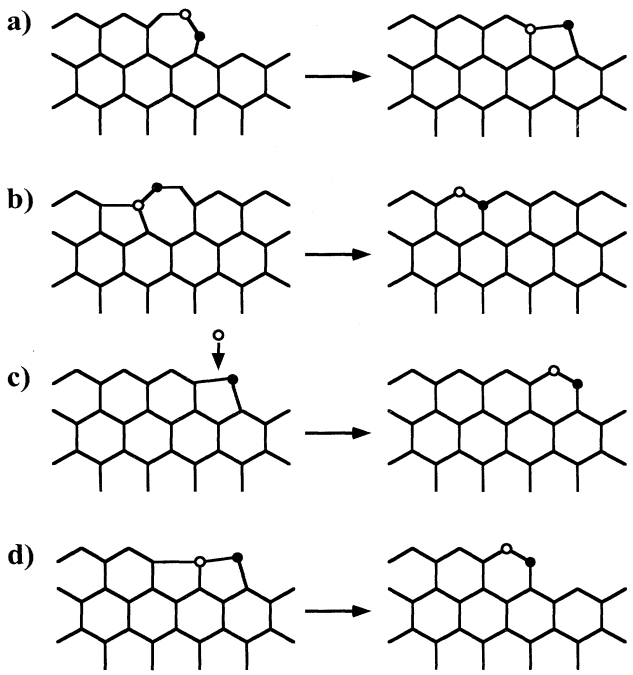

FIG. 7. The various ways in which heptagons and pentagons "anneal" to result in defect-free growth: (a) A heptagon at a step edge breaks up into a pentagon and a hexagon; (b) a heptagon "annihilates" with a pentagon to form a hexagon pair; (c) a pentagon converts to a hexagon by a direct insertion of a deposited atom; (d) a pair of adjacent pentagons at a step edge "fuses" together into a single hexagon.

TABLE I. Energies (in eV) of basic adatom structures that form on the tip of the tube during growth. The energies of even structures are given relative to "6" and of odd configurations relative to "5". See text for an explanation of structure notation.

Structures	1.0 nm (11,3)	2.0 nm (22,5)	3.0 nm (35,5)	4.0 nm (48,6)	6.0 nm (72,6)
			Even configurations		
6	0.000	0.000	0.000	0.000	0.000
55	−0.437	−0.164	0.011	0.116	0.174
565	−0.677	−0.404	−0.204	−0.091	−0.001
5665	−0.711	−0.444	−0.305	−0.141	−0.087
75	0.719	0.773	0.775	0.803	0.789
57	0.503	0.601	0.622	0.661	0.645
576	0.676	0.862	0.903	0.946	0.946
756	0.716	0.783	0.799	0.830	0.813
765	1.041	1.231	1.303	1.339	1.320
567	0.782	1.086	1.186	1.269	1.284
			Odd configurations		
5	0.000	0.000	0.000	0.000	0.000
56	−0.050	0.011	0.047	0.087	0.102
566	0.009	0.078	0.123	0.167	0.211
5666	−0.029	0.097	0.150	0.175	0.195
7	1.350	1.469	1.505	1.529	1.538
76	1.498	1.676	1.751	1.812	1.566
766	1.457	1.646	1.732	1.795	1.833
7666	1.555	1.655	1.722	1.780	1.841

carbon flux is sufficiently high and the rate of diffusion is high enough, the growth of the outer shells will keep pace with the growth of the inner ones, leading to the formation of a multishelled tube without the need for bond formation between the adjacent shells of the growing tube.[30] This scenerio is supported by the apparent independence of the lengths of the various shells of multishelled tubes synthesized in an arc discharge,[31] as well as by the varying number of shells per nanotube. Note that for a complete description of the growth, the initial nucleation stages of the growth still need to be addressed. At this point it is not clear whether growth in the arc discharge is initiated by single- or multiwalled tube fragments.

IV. KINETIC MONTE CARLO SIMULATIONS

The analysis of Sec. III provides an atomistic picture of why wider tubes should grow and narrower ones should close. However, because of the small time step of our MD simulations (0.5 fs) the total simulation time is limited to only several tens of nanoseconds. This makes the growth simulation of even a single layer of a nanotube wider than 3 nm very demanding computationally, even at a relatively high temperature of 3000 K, and simulations at lower temperatures (<2000 K) are presently unfeasible.

In order to extend the total simulation time by four to six orders of magnitude it is necessary to use a method with a basic time step that is several orders of magnitude larger than the MD time step. We found from the MD simulations that the basic microscopic processes leading to nanotube growth or closure involve bond switching that occurs on a time scale of 10–100 ps at the tip temperature of 3000 K. We therefore developed a Monte Carlo (MC) procedure to study the various ring migration processes occurring at the tube tip that involve a series of bond switches. The basis of this formalism is the recognition that at any stage of growth a nanotube consists of only hexagonal rings in the "bulk" layers, and mostly hexagonal rings along with a few pentagonal and heptagonal "defect" rings in the "surface" layer at the tip. All the bond-switching action takes place at the surface layer, and thus the problem scales with the diameter of the tube as (n_1+n_2), where (n_1,n_2) is the tube helicity, and not with the total number of atoms included in the simulation. We exploit the one-to-one correspondence between the number of dangling bonds (the chemically "active" sites) and the number of rings in the surface layer, and treat the rings as the basic units in the MC transitions. The hexagonal rings are thus considered to be the sites with an occupation number of 0, while the pentagons and heptagons are considered to be sites with occupation numbers -1 and $+1$, respectively. The formation of octagons (occupation number of $+2$) by the insertion of an adatom into an existing heptagon is allowed in our simulations, although these immediately break up into smaller rings. In this representation, a single bond switch involves a "flow" of occupation from one ring to its neighbor, with the flow probability governed by the Metropolis algorithm. The total occupation in a single MC step remains constant unless (a) there is an addition of an atom; (b) a new ring is formed at a step edge; or (c) an existing ring is annihilated at a step edge. The energy difference between any two neighboring configurations, involved in a MC move, is expressed as the difference between two appropriate energy variables among the 15 variables listed in the first column of Table I. The notation is in terms or ring sizes, with the rightmost ring at a step edge. Thus "6" denotes an all-hexagonal ring, "57" a pentagon-heptagon pair with the heptagon at a step

edge, "766" a heptagon that is two hexagons away from a step edge, "5" an isolated pentagon at a step edge, and so on. The energies are measured with respect to the all-hexagonal structures for the even configurations, and an isolated pentagon at a step edge for the odd configurations. Note that the "55" configuration changes sign as a function of tube diameter. This occurs at ~3.0 nm, which determines the critical diameter separating tubes that do and do not grow. A general configuration at the tube tip is expressed as a linear combination of the configurations shown in Table I. In the simulations, the structure of the growing nanotube is relaxed by the conjugate gradient method every ten MC steps.

The top views of the resulting tubes of various helicities and diameters are shown in Fig. 8. These structures were obtained after annealing for 5000 MC steps, which roughly corresponds to a total growth time of 250 ns. Narrow tubes clearly start forming caps and close with subsequent deposits. A growth sequence of a (35,5) tube (diameter ~3 nm) is shown in Fig. 9. Note that at different stages of growth the pentagons and heptagons vary in number. However, for all the tubes we have considered (up to a diameter of 6 nm), the numbers of pentagons and heptagons are very low at all times of growth. The number of pentagons rarely exceeds 6 and the number of heptagons almost never exceeds 2. Therefore the wider tubes always remain straight and grow with a net addition of hexagonal rings at the step edges.

The ability to carry out long simulations with MC allows us to estimate the minimum temperature needed for nanotube growth. For this, one first needs to calculate the fastest growth rate as a function of temperature. Assuming Arrhenius behavior, the average time τ_{switch} in which a bond switching occurs at a temperature T is given by the formula $\tau_{\text{switch}}=\tau_0\exp(\Delta/k_BT)$, where τ_0 is the average time scale of the *attempt* of a single bond switch, Δ is a typical barrier encountered in a bond switch, and k_B is the Boltzmann constant. If a minimum of N_{MC} local bond switches is required for full annealing of defects, an interval of at least $\tau_{\text{min}}=N_{\text{MC}}\tau_0\exp(\Delta/k_BT)$ is mandated between successive deposits at the same site of the tube tip, in order to ensure defect-free growth. The fastest growth rate γ at a temperature T is thus estimated by the formula

$$\gamma=\delta_{\text{layer}}/\tau_{\text{min}}=\delta_{\text{layer}}(N_{\text{MC}}\tau_0)^{-1}\exp(-\Delta/k_BT)\ , \qquad (1)$$

where δ_{layer} is the average height of a nanotube layer ~1.0 Å. From MD simulations at 3000 K we obtain $\tau_0\sim0.1$ ps, $\tau_{\text{switch}}\sim50$ ps, and $\Delta\sim1.55$ eV. From extensive MC simulations we obtain $N_{\text{MC}}\sim50$. The resulting values of γ for various temperatures are shown in Table II. Considering that experimental growth rates lie in the

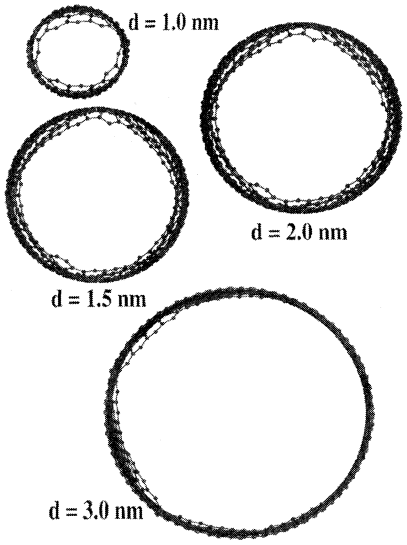

FIG. 8. Top view of tubes of various diameters annealed by 5000 MC time steps at 3000 K. Narrow tubes are clearly going to close.

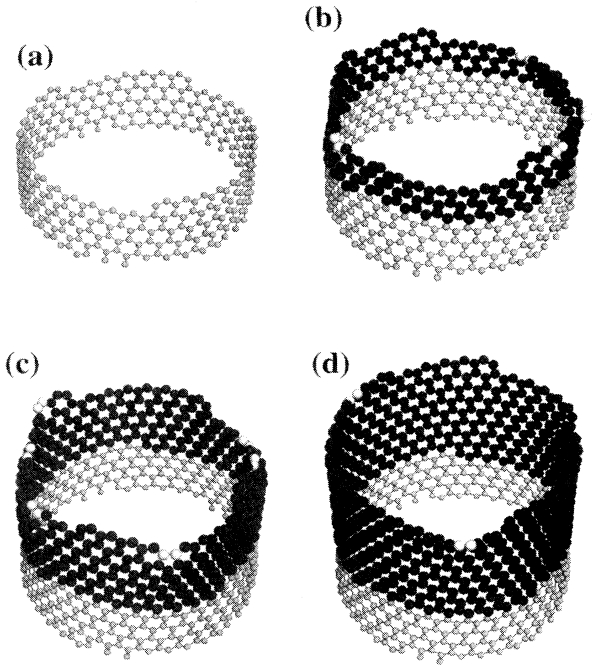

FIG. 9. A growth sequence of a 3-nm-wide tube of helicity (35,5): (a) the initial all-hexagonal tube; (b) after the addition of 200 atoms; (c) after 400 atoms; and (d) after 600 atoms. The number of pentagons and heptagons are 3 and 1 in (b), 5 and 1 in (c), and 1 and 1 in (d), respectively. Their positions are high lighted by the lighter atoms at the tube tips.

TABLE II. Fastest growth rate of a nanotube as a function of temperature. Experimental rates are between 1 and 500 Å/ms. See text.

Temperature (K)	Fastest growth rate (Å/ms)
3000	4.0×10^5
2500	1.2×10^5
2000	1.9×10^4
1500	8.2×10^2
1000	1.6×10^0
500	$\ll1.0$

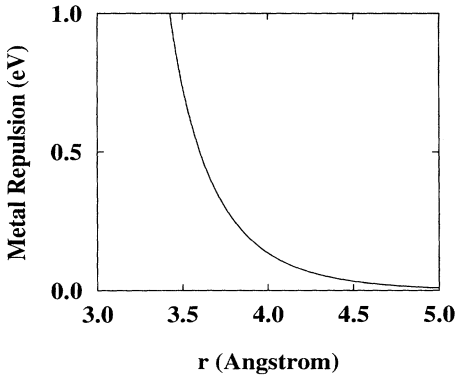

FIG. 10. Plot of the cylindrically symmetric repulsive potential used to represent the catalytic metal particle, as a function of the radial distance from the tube axis. The radius of the hard core is 3 Å and the tube radius is 5 Å.

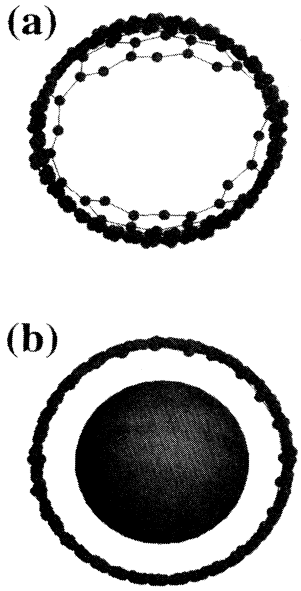

FIG. 11. Top view of a 1.0-nm-diam tube in the absence (a) and presence (b) of a metal particle. The tube (a) closes while tube (b) grows.

range 1–500 Å/ms,[16,32] a minimum temperature of ~1000 K is mandated by our tube growth mechanism. Although it is difficult to estimate experimental temperatures at the tube tip, this value seems to be consistent with all arc discharge experiments.

As described above, growth simulations by both molecular dynamics and Monte Carlo on tubes narrower than a critical diameter ~3 nm lead to the closure of the tube and cessation of growth. However, very recently, nanotubes of diameter as small as ~0.8 nm have been grown in arc discharge in the presence of transition metal catalysts.[15] In order to shed some light on the growth mechanism of these very narrow tubes, we have performed MC simulations of their growth in the presence of metal particles inside the tube. The presence of a metal catalyst was represented by a coaxial hard shell with a radial repulsive potential V_m of the Yukawa form:

$$V_m(r)=V_0\frac{\exp[-\lambda(r-r_c)]}{r-r_c} \quad \text{for } r>r_c\ , \tag{2}$$

where r is the radial distance from the tube center, r_c is the radius of the hard shell (~2 Å less than the tube radius), λ is the inverse of the screening length, and V_0 sets the energy scale for the potential. We have carried out MC simulations on a 1.0-nm-diam tube in the presence of such a potential with $V_0=1.0$ eV Å, $\lambda=2.0$ Å^{-1}, and $r_c=3.0$ Å, which corresponds to a potential of only 10 meV at the tube radius (Fig. 10). The resulting tubes annealed by MC without and width this potential are shown in Fig. 11. The tube remains straight and defect-free in the presence of the potential, while the tip curves up immediately if no potential is present.

While this picture of metal catalytic growth is somewhat simplistic, the results clearly show that small metal particles can indeed prevent the closure of narrow carbon nanotubes and lead to growth. A more detailed investigation of the formation of nanotubes on metal particles is currently underway.

V. SUMMARY

In summary, we have studied the kinetics of carbon nanotube growth in a standard arc discharge geometry with a variety of complementary numerical techniques. An accurate calculation of the electric field present at the tips of both open and closed tubes followed by *ab initio* MD simulation shows that the electric field cannot be the critical factor responsible for open-ended growth. The mechanism of growth was therefore investigated further by classical MD and kinetic MC simulations, using realistic, many-body potentials. Wide, helical tubes are found to grow by the net addition of hexagons at the step edges. This addition occurs when various nonhexagonal ring structures (pentagons, heptagons, and octagons), which may form initially upon the deposition of atoms or small clusters, combine and annihilate into hexagons. All-hexagonal structures, once formed, are quite stable against bond-switching processes even at high temperatures. The pentagons and heptagons are always few in number and well distributed after annealing. However, adjacent pentagonal structures nucleate quite readily on the narrow tubes, resulting in structures that are highly curved and lead to tube closure with further addition of atoms. Our attempts to grow an already closed tube by depositing atoms onto its cap result only in the formation of a disordered tip. The above results are in agreement with the open-ended growth model[10] and also explain the absence of narrow tubes under conditions of noncatalytic growth.[8] Once an open-ended tube forms and grows, other shells are expected to form, using the surface of the

nanotube as a template. This readily leads to the formation of multishelled tubes in the arc discharge apparatus. Finally, the growth of very narrow tubes in the presence of a metal particle[15] was simulated by modeling the particle with a repulsive hard core coaxial with the tube. For a tube of diameter 1.0 nm, we have shown that even a potential as small as 10 meV at the position of tube atoms is strong enough to "straighten" the tube that would otherwise curve and eventually close. The resultant tube behaves just like a wide tube in noncatalytic growth and can grow straight and defect-free.

ACKNOWLEDGMENTS

This work was supported by the Office of Naval Research Grant No. N00014-91-J-1516. Some of the calculations were carried out at the North Carolina Supercomputing Center.

[1]H. W. Kroto, J. R. Heath, S. C. O'Brien, R. F. Curl, and R. E. Smalley, Nature (London) **318**, 162 (1985).
[2]W. Kratschmer, L. D. Lamb, K. Fostiropoulos, and D. R. Huffman, Nature (London) **347**, 354 (1990).
[3]R. Ettl, I. Chao, F. Diederich, and R. L. Whetten, Nature (London) **353**, 149 (1991).
[4]F. Diederich, R. Ettl, Y. Rubin, R. L. Whetten, R. Beck, M. Alvarez, S. Arz, D. Sensharma, F. Wudl, K. L. Khemani, and A. Koch, Science **252**, 548 (1991).
[5]K. Kikuchi, N. Nakahara, T. Wakabyashi, S. Suzuki, H. Shinonamaru, M. Miyake, K. Saito, I. Ikemoto, M. Kainosho, and Y. Achiba, Nature (London) **354**, 56 (1991).
[6]D. Ugarte, Nature (London) **359**, 707 (1992).
[7]D. Ugarte, Europhys. Lett. **22**, 45 (1993).
[8]S. Iijima, Nature (London) **354**, 56 (1991).
[9]T. W. Ebbesen and P. M. Ajayan, Nature (London) **358**, 220 (1992).
[10]S. Iijima, P. M. Ajayan, and I. Ichihashi, Phys. Rev. Lett. **69**, 3100 (1992).
[11]P. Calvert, Nature (London) **357**, 365 (1992).
[12]P. Ross, Sci. Am. **265**, 16 (1991).
[13]J. Broughton and M. Pederson, Phys. Rev. Lett. **69**, 2689 (1992).
[14]N. Hamada, S. Sawada, and A. Oshiyama, Phys. Rev. Lett. **68**, 1579 (1992); J. W. Mintmire, B. I. Dunlap, and C. T. White, *ibid.* **68**, 631 (1992); R. Saito, M. Fujita, G. Dresselhaus, and M. S. Dresselhaus, Appl. Phys. Lett. **60**, 2204 (1992).
[15]S. Iijima and T. Ichihashi, Nature (London) **363**, 603 (1993); D. S. Bethune, C. H. Kiang, M. S. de Vries, G. Gorman, R. Savoy, J. Vazquez, and R. Beyers, *ibid.* **363**, 605 (1993); Y. Saito, M. Okuda, N. Fujimoto, T. Yoshikawa, M. Tomita, and T. Hayashi, Jpn. J. Appl. Phys. **33**, L526 (1994); S. Seraphin, J. Electrochem. Soc. **142**, 290 (1995).
[16]N. Hatta and K. Murata, Chem. Phys. Lett. **217**, 398 (1994).
[17]M. Endo and H. W. Kroto, J. Phys. Chem. **96**, 6941 (1992); R. Saito, G. Dresselhaus, and M. S. Dresselhaus, Chem. Phys. Lett. **195**, 537 (1992).
[18]R. E. Smalley, Mater. Sci. Eng. B **19**, 1 (1993).
[19]J. D. Cobine, *Gaseous Conductors* (Dover, New York, 1958).
[20]A. M. Winslow, J. Comput. Phys. **2**, 2149 (1967); K. Halbach, Nucl. Instrum. Methods **66**, 154 (1968); M. T. Menzel and H. K. Stokes, computer code POISSON, Los Alamos National Laboratory, Los Alamos, NM.
[21]R. Car and M. Parrinello, Phys. Rev. Lett. **66**, 2633 (1991).
[22]G. Li and S. Rabii (unpublished).
[23]J. C. Perdew and A. Zunger, Phys. Rev. B **23**, 5048 (1981).
[24]Recent galvanomagnetic measurements indicate that bundles of nanotubes formed in an arc discharge are mostly semimetallic; see S. N. Song, X. K. Wang, R. P. H. Chang, and J. B. Ketterson, Phys. Rev. Lett. **72**, 697 (1994).
[25]P. Nordlander (private communication).
[26]J. Tersoff, Phys. Rev. Lett. **56**, 632 (1986); **61**, 2879 (1988); Phys. Rev. B **37**, 6991 (1988).
[27]D. W. Brenner, in *Atomic Scale Calculations in Materials Science,* edited by J. Tersoff, D. Vanderbilt, and V. Vitek, MRS Symposia Proceedings No. 141 (Materials Research Society, Pittsburgh, 1989), p. 59; Phys. Rev. B **42**, 9458 (1990).
[28]A. Maiti, C. J. Brabec, C. Roland, and J. Bernholc, Phys. Rev. Lett. **73**, 2468 (1994).
[29]C. J. Brabec, A. Maiti, C. Roland, and J. Bernholc, Chem. Phys. Lett. **236**, 150 (1995).
[30]T. Guo, P. Nikolaev, A. G. Rinzler, D. Tomanek, D. T. Colbert, and R. E. Smalley, J. Phys. Chem. **99**, 10 694 (1995).
[31]S. Iijima (unpublished).
[32]P. Byszewski, K. Ukalski, M. Baran, P. Dluzewski, and M. Kozlowski (unpublished).

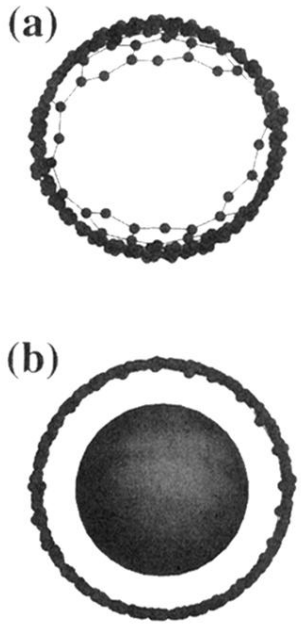

FIG. 11. Top view of a 1.0-nm-diam tube in the absence (a) and presence (b) of a metal particle. The tube (a) closes while tube (b) grows.

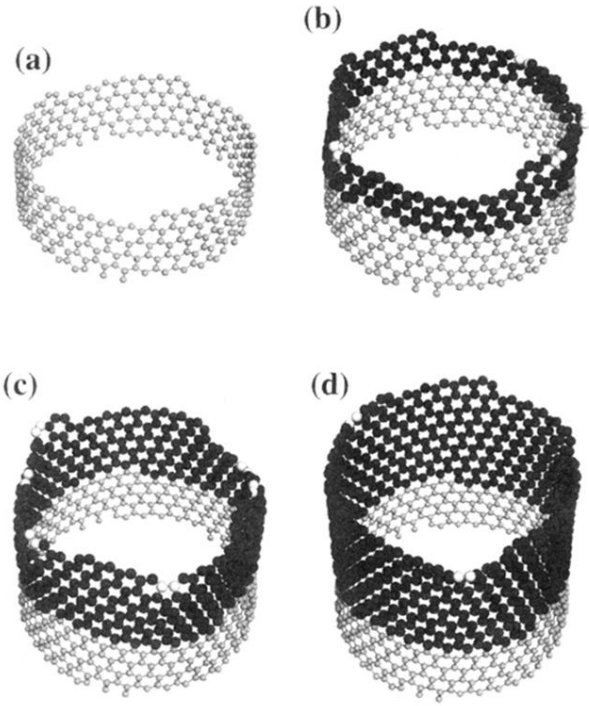

FIG. 9. A growth sequence of a 3-nm-wide tube of helicity (35,5): (a) the initial all-hexagonal tube; (b) after the addition of 200 atoms; (c) after 400 atoms; and (d) after 600 atoms. The number of pentagons and heptagons are 3 and 1 in (b), 5 and 1 in (c), and 1 and 1 in (d), respectively. Their positions are high lighted by the lighter atoms at the tube tips.